IVYSPRING INTERNATIONAL PUBLISHER

Theranostics

2025; 15(3): 1017-1034. doi: 10.7150/thno.102671

Review

Optical molecular imaging technology and its application in precise surgical navigation of liver cancer

Pan He[1,3#], Haitian Tang[2#], Yating Zheng[2], Xiao Xu[2], Xuqi Peng[2], Tao Jiang[3], Yongfu Xiong[3], Yang Zhang[2], Yu Zhang[1✉], Gang Liu[2✉]

1. Department of Hepatobiliary and Pancreas Surgery, Sichuan Provincial People's Hospital, University of Electronic Science and Technology of China, Chengdu 611731, China.
2. State Key Laboratory of Vaccines for Infectious Diseases, Center for Molecular Imaging and Translational Medicine, Xiang An Biomedicine Laboratory, National Innovation Platform for Industry-Education Integration in Vaccine Research, School of Public Health, Xiamen University, Xiamen 361002, China.
3. Department of General Surgery, Institute of Hepatobiliary-Pancreatic-Intestinal Diseases, Affiliated Hospital of North Sichuan Medical College, Nanchong 637000, China.

# P. He, and H. Tang contributed equally to this work.

✉ Corresponding authors: gangliu.cmitm@xmu.edu.cn (Gang Liu), zhangyuqg@med.uestc.edu.cn (Yu Zhang).

Received: 2024.08.22; Accepted: 2024.11.30; Published: 2025.01.01

Abstract

Recent innovations in medical imaging technology have placed molecular imaging techniques at the forefront of diagnostic advancements. The current research trajectory in this field aims to integrate personalized molecular data of patients and diseases with traditional anatomical imaging data, enabling more precise, non-invasive, or minimally invasive diagnostic options for clinical medicine. This article provides an in-depth exploration of the basic principles and system components of optical molecular imaging technology. It also examines commonly used targeting mechanisms of optical probes, focusing especially on indocyanine green—the FDA-approved optical dye widely used in clinical settings—and its specific applications in diagnosing and treating liver cancer. Finally, this review highlights the advantages, limitations, and future challenges facing optical molecular imaging technology, offering a comprehensive overview of recent advances, clinical applications, and potential impacts on liver cancer treatment strategies.

Keywords: Molecular imaging; Theranostics; Liver cancer; Surgical navigation

Introduction

Advancements in imaging technologies have significantly accelerated the development of molecular imaging, reshaping diagnostic and treatment paradigms in clinical medicine [1,2]. Molecular imaging uses two- and three-dimensional imaging devices to capture and differentiate various physiological and pathological processes at the cellular and even subcellular levels *in vivo*. This approach enables qualitative and quantitative analyses, providing highly sensitive detection methods to facilitate early disease diagnosis [3]. Unlike traditional imaging, which primarily visualizes structural abnormalities, molecular imaging leverages biochemical and intracellular pathways to illuminate disease initiation and progression mechanisms [4]. As research into molecular disease mechanisms has deepened, the potential of molecular imaging to enhance clinical understanding and treatment strategies has advanced, driving its rapid integration into both foundational and clinical disease research.

In clinical practice, molecular imaging is increasingly valued for its ability to assess cellular-level changes that often precede detectable anatomical alterations, thus aiding in early diagnosis and disease characterization [5-7]. This approach is particularly adept at identifying functional changes within tissues, enhancing sensitivity over traditional

imaging modalities. Additionally, molecular imaging has proven invaluable for early-stage drug evaluation, allowing researchers to precisely and quantitatively monitor the effects of drugs on molecular targets *in vivo* [8]. In gene therapy, molecular imaging facilitates the detection of genetic-level changes, enabling the real-time monitoring of disease onset and progression before phenotypic alterations become evident.

In summary, molecular imaging is an interdisciplinary field encompassing various imaging modalities, such as positron emission tomography and single-photon emission computed tomography, both rooted in nuclear medicine, as well as imaging based on nuclear magnetic resonance and optical molecular imaging techniques [9]. In recent years, optical molecular imaging has emerged as a promising modality for cancer diagnosis and treatment, particularly in enhancing precision surgery. However, the complexity of visualizing anatomical structures and physiological functions in this modality presents challenges in designing high-quality imaging systems and developing targeted probes, which impacts the clinical translation of applications [10]. Based on current optical imaging systems and strategies [11], this review (**Figure 1**) delves into the fundamental principles and components of optical molecular imaging. Furthermore, it examines common targeting mechanisms of optical probes, emphasizing indocyanine green (ICG), a Food and Drug Administration (FDA)-approved optical dye for clinical applications, specifically for diagnosing and treating liver cancer. Lastly, the review discusses the benefits, limitations, and future challenges of optical molecular imaging.

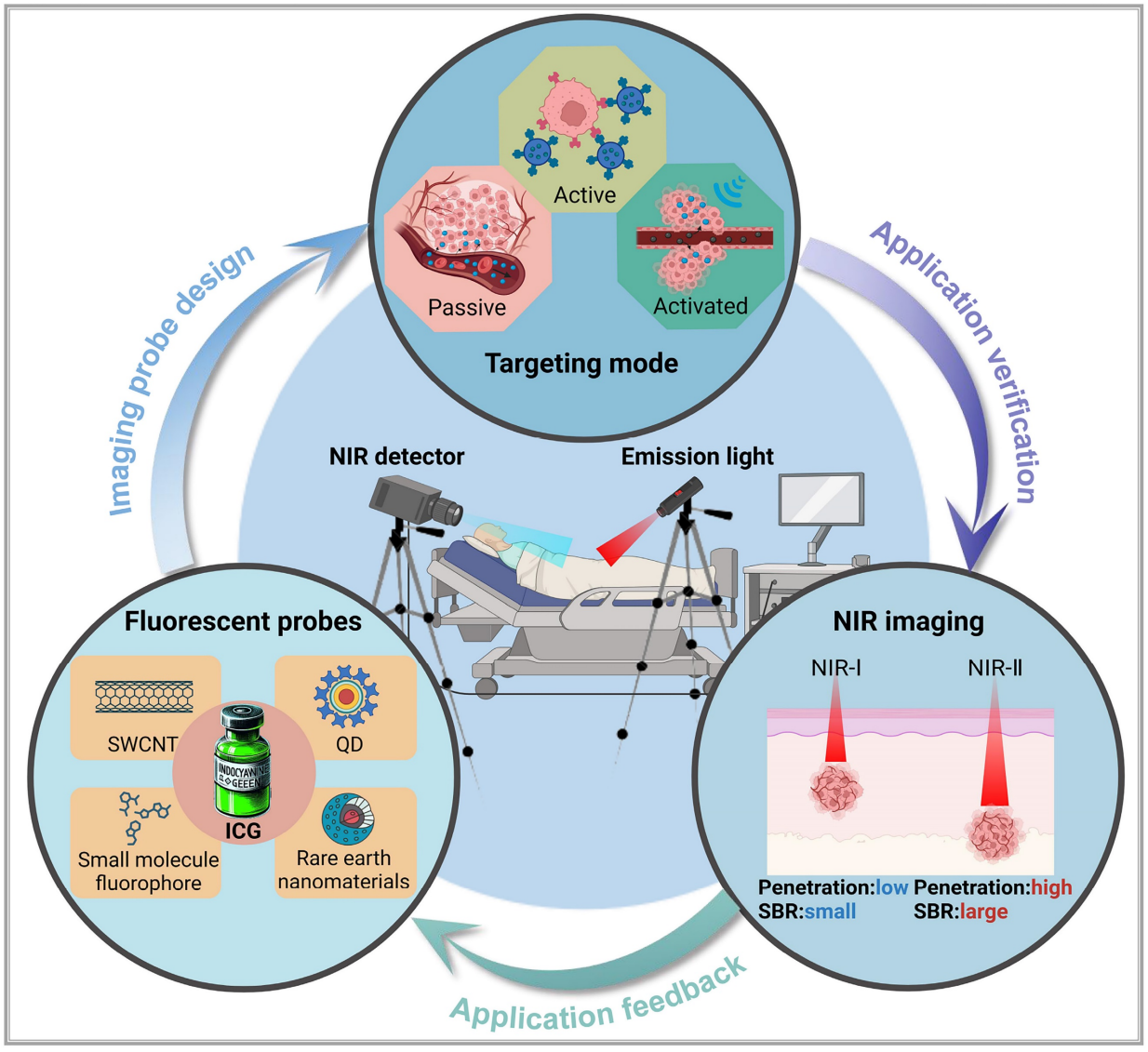

Figure 1. An illustration that represents optical molecular imaging techniques and their key applications in precision surgery navigation, including common fluorescent probes, an introduction to the targeting methods of probes, and a comparison of NIR-I and NIR-II imaging. SWCNT = Single-walled carbon nano tube, QD = Quantum dot. This figure was created with Biorender.com.

Optical molecular imaging technology

Optical molecular imaging is a non-invasive, real-time, and high-resolution imaging modality that combines optical technology with biomolecular labeling. It detects light signals emitted by endogenous or exogenous agents in tissues and translates cellular activities into visual patterns through specialized optical imaging devices [12]. The main components of an optical molecular imaging system include the luminescent signal source, light source transmission and positioning systems, and the optical signal reception and analysis systems. The following detailed review provides an overview of these components.

Luminous signal source of the imaging system

Optical molecular imaging systems rely on diverse luminescent signal sources with significantly varying biological and optical characteristics, requiring careful selection based on specific applications [13]. In general, luminescent sources in optical imaging systems fall into two categories: endogenous and exogenous signals. Endogenous signals are directly related to living organisms, such as electronic energy transitions generated by biochemical reactions within the body, energy transitions triggered by external radiation or internal biochemical processes [14], for example, organisms such as fireflies naturally produce luminescence from biochemical reactions [15]. However, in humans, spontaneous luminescence is relatively weak and lacks contrast against the background, making it difficult to distinguish effectively and unsuitable as a light source for optical imaging technology. Additionally, this signal can interfere with imaging data, affecting the detection results of the imaging system. Therefore, specific measures are often required in optical molecular imaging to eliminate or suppress the inherent luminescence of tissues to obtain clearer imaging results. The second category involves exogenous signals produced by luminescent materials, such as fluorescent dyes [16], fluorescent proteins [17], and quantum dots [18], either through spontaneous emission or light stimulation.

In developing optical biological probes, the luminescent material is crucial for probe distribution and imaging contrast. Although numerous fluorescent materials are available, only a very few are FDA-approved for human use, including ICG, sodium fluorescein, pafolacanine, and methylene blue [19,20]. Among them, ICG is widely recognized for its unique advantages in clinical imaging. Specifically, ICG's emission of near-infrared (NIR) light improves imaging contrast by operating outside the body's natural luminescence spectrum. Additionally, NIR light has lower absorption and scattering in tissues, allowing deeper tissue penetration [21,22]. Beyond these benefits, ICG demonstrates exceptional utility for imaging in both the first and second NIR regions, making it particularly valuable in liver cancer imaging.

Common targeting methods for optical molecular imaging

To achieve precise imaging of the target areas, it is necessary to first accurately deliver luminescent materials to specific target points and then emit light signals. Depending on the use of carriers and their characteristics, the delivery of luminescent dyes to the target areas can be categorized into three: passive targeting, active targeting, and *in situ* activated probes (**Figure 2**).

Passive targeting

The most well-known theory in the passive targeting mechanism is the Enhanced Permeability and Retention (EPR) effect, which relies on the permeability of specific tissues or organs, guiding large molecular substances (such as nanoparticles and liposomes) to naturally accumulate in non-specific diseased tissues within the body. The mechanism of this effect can be attributed to two factors: (I) the disorganized structure and discontinuous endothelium of tumor neovasculature leading to excessive permeability of large molecules, and (II) the lack of an effective lymphatic drainage system in the tumor region, which causes accumulation of large molecular substances in that area [23,24]. Fluorescent substances with passive targeting capabilities are generally composed of one or more luminescent materials to form a macromolecular contrast agent. After injection into the body, they do not bind to targeting ligands, rather directly enter the body, mainly in the blood. Therefore, regions with rich blood supply (vessels, high metabolic areas, and tumor neovasculature) appear as bright areas. This method is commonly employed in vascular and urinary tract imaging studies among others. Indeed, these macromolecules can also leak out into diseased tissues through incomplete or damaged vascular endothelial gaps, aiding visualization. ICG, for example, has been clinically applied in ophthalmic optical imaging technology for over 40 years through this approach [25]. Moreover, experimental evidence has demonstrated that ICG achieves optical imaging of certain tumors through these non-specific means [19,20]. Particularly, as ICG is exclusively cleared through the liver, it exhibits specific accumulation in liver cancer tissues, thereby providing a new method

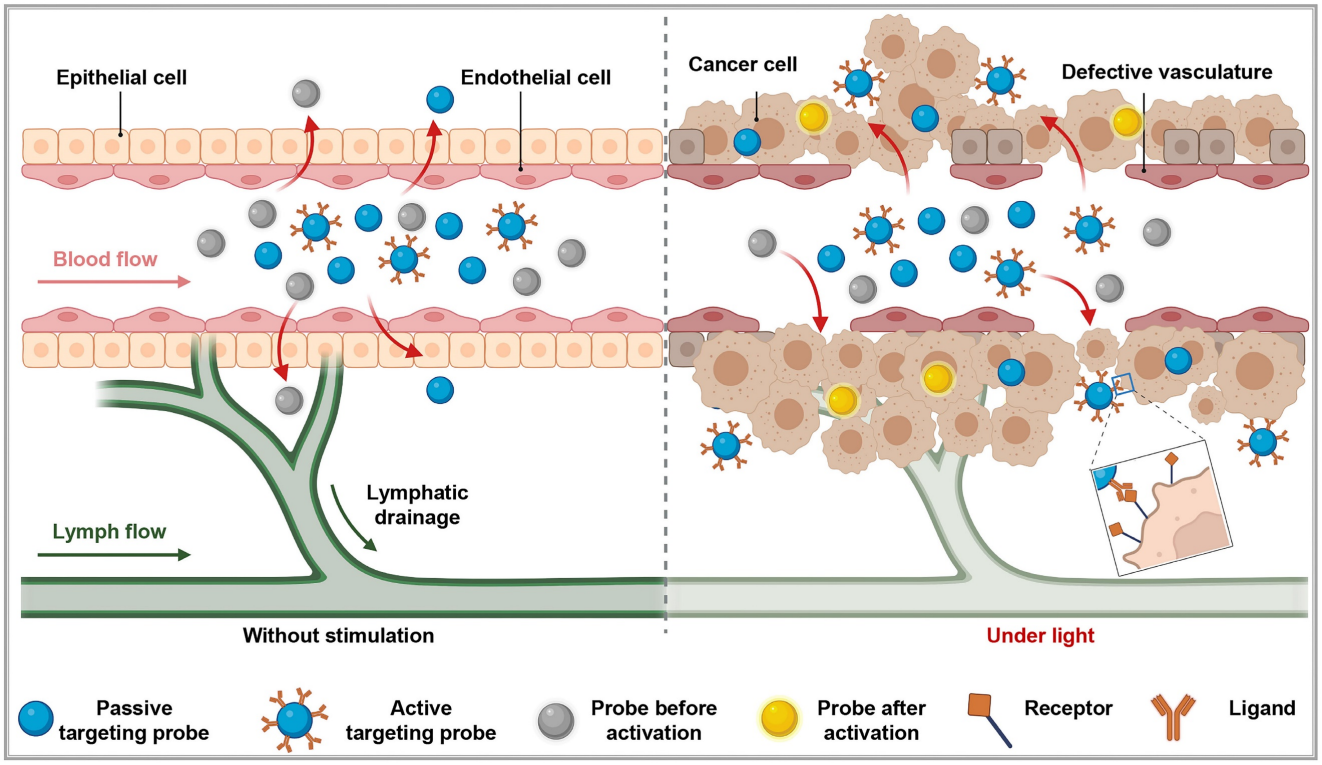

Figure 2. Three principal targeting strategies for nanoprobes: In the absence of an external excitation source, active targeting probes do not migrate from blood vessels into surrounding tissues. Some passive targeting and activatable probes can enter surrounding tissues via the enhanced permeability and retention effect. However, under these conditions, activatable probes lack drug activity (depicted as gray). When pathological changes, such as cancer, occur in the surrounding tissues, active targeting probes can specifically target and penetrate the diseased area. Meanwhile, activatable probes exhibit drug activity (depicted as yellow) under the influence of an external excitation source. This figure was created with Biorender.com.

for the diagnosis and surgical treatment of liver cancer [26].

While the EPR effect demonstrates notable results in animal models, its effectiveness in clinical settings often falls short, raising questions related to its existence and prompting the exploration of new mechanisms to explain the passive targeting effects of nanomedicines. Sindhwanni [27] proposed that endocytosis might be the primary mechanism for the accumulation of nanoparticles at the tumor sites. They adopted the "Zombie" model to distinguish between passive penetration and active transport through endothelial cells, attempting to determine the dominant mechanism for nanoparticle accumulation in the tumor tissues. Simultaneously, Wang [28] suggested that the basement membrane around tumor blood vessels forms a barrier that hinders the penetration of nanodrugs through the tumor vascular wall. The authors demonstrated that the subendothelial space formed between the basement membrane surrounding tumor blood vessels and endothelial cells serves as a barrier where nanoparticles are intercepted, thereby forming a "subendothelial nanoparticle pool." This basement membrane barrier not only hinders the penetration of nanoparticles into deeper layers of tumor tissues but also restricts their ability to pass through the inter-endothelial gaps of endothelial cells. The synergistic immune-driven strategy induced by local hyperthermia overcomes this barrier and enhances the delivery of nanotherapies to tumors.

Active targeting

Active targeting probes in biomedicine are composed of highly specific ligands coupled with fluorescent markers, allowing for precise recognition and binding to target tissues. By combining fluorescent markers with targeting ligands, these biologically targeted probes offer advanced recognition capabilities, enabling specific imaging of molecular targets [29]. Compared to passive targeting techniques, active targeting probes reflect the expression levels of target molecules more accurately by measuring fluorescent signal intensity. This high specificity minimizes interference from non-specific factors such as tumor microenvironment variability or vascular permeability changes [30]. Active targeting ligands are diverse and not limited to antibodies [31]; they also include small molecules [32], short peptide sequences [33], nucleic acid aptamers [34], proteins, and others [35,36]. Each type of ligand has distinct advantages and limitations, allowing for tailored probe selection based on specific imaging requirements. However, the prolonged half-life of

ligand-fluorescent probes can sometimes reduce image clarity, as background signals may compete with target signals [37]. To enhance imaging contrast, two strategies can be employed: introducing a molecule after probe binding to the target, which binds to unbound probes in the bloodstream and promotes clearance, and applying fluorescence resonance energy transfer technology, where a molecule binds to the unbound probe, inducing fluorescence quenching to minimize non-specific signals [38].

With the distinctive capabilities of nanomedicine in cancer diagnosis and treatment, researchers have developed actively targeted probes that attach to specific biomarkers by precisely modifying nanocarrier surfaces [39]. These advancements allow for early disease diagnosis, real-time monitoring of disease progression, and assessment of therapeutic effectiveness. For example, the Bevacizumab-IRDye 800CW and Angiostamp800 probes, developed by Hurbin, provide superior tumor detection and are resistant to rapid clearance by the body [40]. Swamy expanded on this approach by designing a π-conjugated ICG derivative paired with a monoclonal antibody to image human epidermal growth factor receptor 2- and epidermal growth factor receptor-positive breast cancers in patients, achieving promising results. Compared to traditional ICG, these specific fluorescent probes enable more accurate detection of tumors and metastatic sites, facilitating precise tumor resections [41]. In another example, Shi labeled a humanized anti-GPC3 monoclonal antibody with ICG to create a NIR-II fluorescent probe (GPC3-ICG) designed to specifically target hepatocellular carcinoma (HCC) (**Figure 3A**). GPC3-ICG demonstrated high specificity and uptake in HCC cell lines (Huh-7, Hep G2, Hep 3B), exhibiting excellent efficiency and specificity (**Figure 3B-C**) [42].

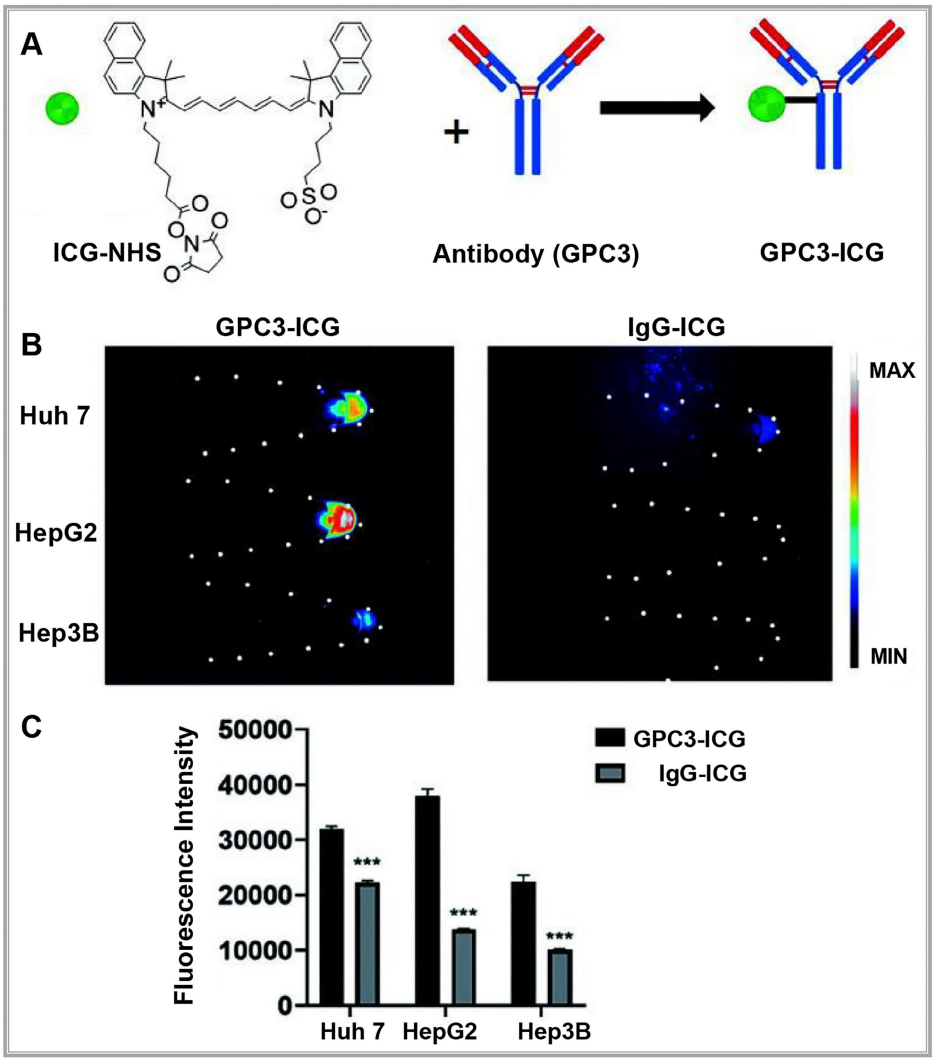

Figure 3. (A) NIR-II imaging of hepatocellular carcinoma based on a humanized anti-GPC3 antibody. **(B)** Different probes (left GPC3-ICG, right IgG-ICG) were incubated with Huh-7, Hep G2, and Hep 3B cell lines, and NIR-II images of the cell pellets were captured. **(C)** Quantification analysis of the NIR-II fluorescence intensity in different cell lines. The error bars indicate mean ± SD, $^{**}p < 0.01$ with two-tailed Student's t-test. Reproduced with permission from [42], copyright 2022, Royal Society of Chemistry.

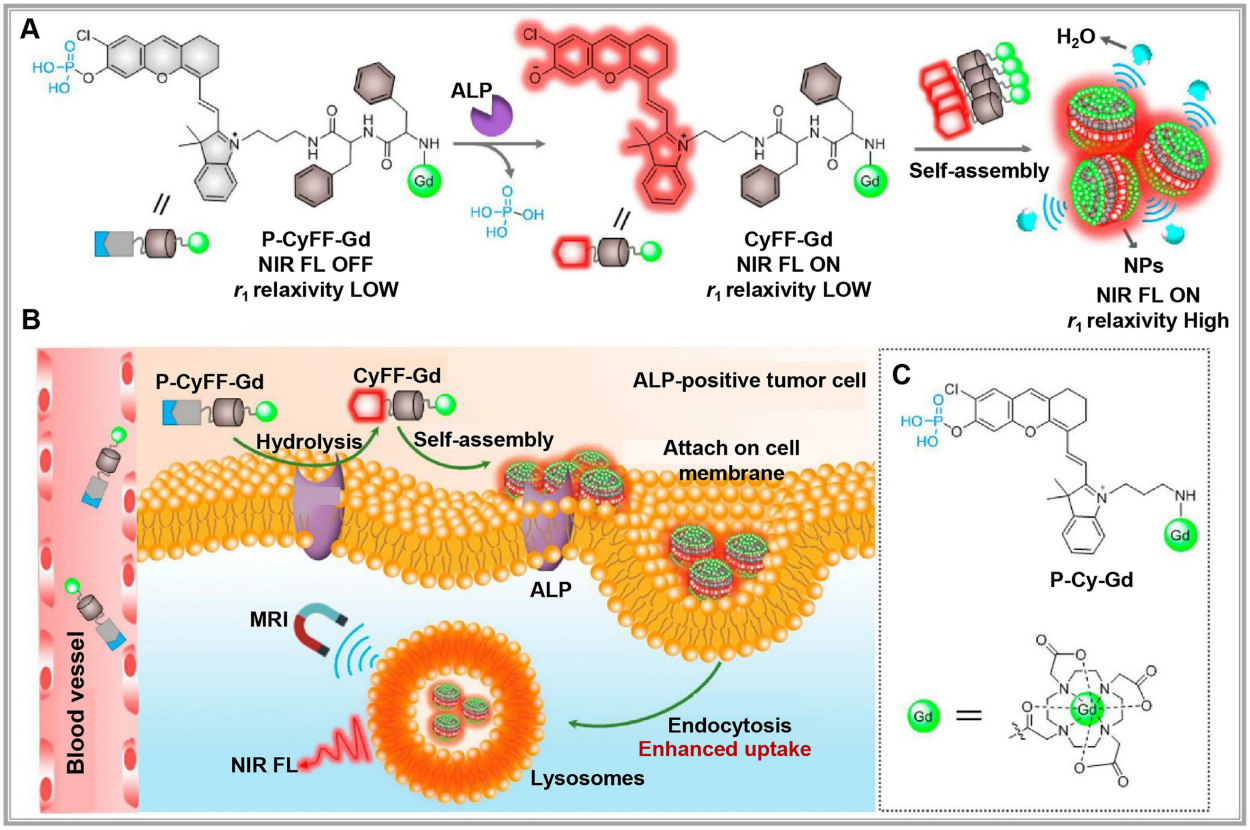

Figure 4. (A) Chemical structure of P-CyFF-Gd and proposed alkaline phosphatase (ALP)-mediated fluorogenic reaction and *in situ* self-assembly of P-CyFF-Gd into nanoparticles (NPs) that show increased NIR FL and r1 relaxivity. **(B)** Proposed mechanism of P-CyFF-Gd for NIR FL/MR bimodality imaging of ALP-positive tumor cells *in vivo*. Following systemic administration into mice, P-CyFF-Gd as a small molecule may easily across blood vessel and diffuse into tumor tissues. In tumor cells that express high levels of ALP, P-CyFF-Gd is dephosphorylated by membrane-bound ALP and converted into fluorescent CyFF-Gd, which subsequently selfassembles into fluorescent and magnetic NPs. **(C)** Chemical structure of the designed nonassembled control probe, P-Cy-Gd. Reproduced with permission from [51], copyright 2019, American Chemical Society.

Activating optical probe

Activatable optical probes rely on specific environmental triggers, such as variations in pH, enzyme presence, or light exposure, to activate and enable optical imaging [43]. Typically inactive under normal conditions, these probes are designed to become active and emit signals only upon encountering specific conditions in the target area, providing higher contrast fluorescence imaging compared to "always-on" probes [44,45].

Activatable optical probes fall into two main categories: activatable probes and binding probes. Activatable probes often consist of a fluorophore paired with a quencher, engineered to maintain proximity to precisely control fluorescence signal activation and quenching. For example, a peptide sequence linking the fluorophore and quencher can be tailored to respond to specific protease activities in the target region [46,47]. By contrast, binding probes emit signals upon binding to specific biomarkers [37,48]. For example, in DNA methylation assessment, probes targeting cytosine selectively bind to methylated alleles, emitting a fluorescent signal [49]. Researchers have recently developed new "switch-like" probe strategies [50]. For instance, alkaline phosphatase (ALP)-activated NIR fluorescence and magnetic resonance bimodal probes respond to ALP overexpression on cell membranes, forming nanoparticles visible through cryo-SEM imaging (**Figure 4A**). This bimodal approach enhances NIR fluorescence (>70-fold at 710 nm) and improves r1 relaxivity (~2.3-fold), allowing for real-time, high-sensitivity, high-resolution imaging and localization of ALP activity in live tumor cells and mice (**Figure 4B-C**) [51].

Combined targeting and multimodal imaging strategies

In clinical settings, combining targeted probe delivery with multimodal imaging can significantly increase drug delivery precision and drug concentration at target sites. For example, nano-targeted probes use specific antibodies to actively target lesions and accumulate passively in tumor tissue via the EPR effect, boosting local probe concentration [52]. Additionally, optical probes combined with other imaging modalities can improve diagnostic accuracy and offer better therapeutic guidance, thus overcoming the limitations of single imaging methods. For instance, combining NIR dyes

with gadolinium (Gd)-based nanoparticles enables multimodal MRI and NIR imaging [53,54]. Furthermore, labeling NIR dyes with radioactive isotopes allows for the high sensitivity of PET, SPECT, and fluorescence imaging, facilitating early tumor diagnosis and treatment [55-57].

Precision-guided injections can also enhance targeting when combined with other imaging techniques. For example, ultrasound imaging provides real-time visualization of tissue structure, enabling the precise injection of optical probes into target areas for detailed molecular or cellular imaging [58]. Alternatively, interventional techniques allow optical probes to be directly delivered to tumors via microcatheter superselection of tumor-feeding arteries, thereby increasing the local drug concentration in the tumor and improving imaging accuracy. Our research team has pioneered interventional optical molecular imaging, developing a super-stable homogeneous drug formulation technology that stably combines fluorescent dyes with interventional embolic agents (**Figure 5A**) [59]. This innovation provides a promising approach for integrated diagnosis and treatment of liver cancer (**Figure 5B**) [60].

Optical imaging system

NIR fluorescence imaging offers superior tissue penetration, low cost, high sensitivity, and safety advantages compared with visible light. These qualities make it an invaluable tool for real-time navigation during cancer surgeries [61]. Achieving high-quality optical imaging relies on both a robust imaging system and effective fluorescent probes. Being key components of molecular imaging, fluorescence imaging systems capture light emitted by fluorophores excited by an external light source. This light is transformed by photoelectric conversion devices into digital signals, and then, displayed for the observer. Such systems typically include lenses, filters, electronic coupling devices, or complementary metal-oxide-semiconductor detectors, laser scanning or detection systems, lasers, computers, and biomedical signal processing software [19].

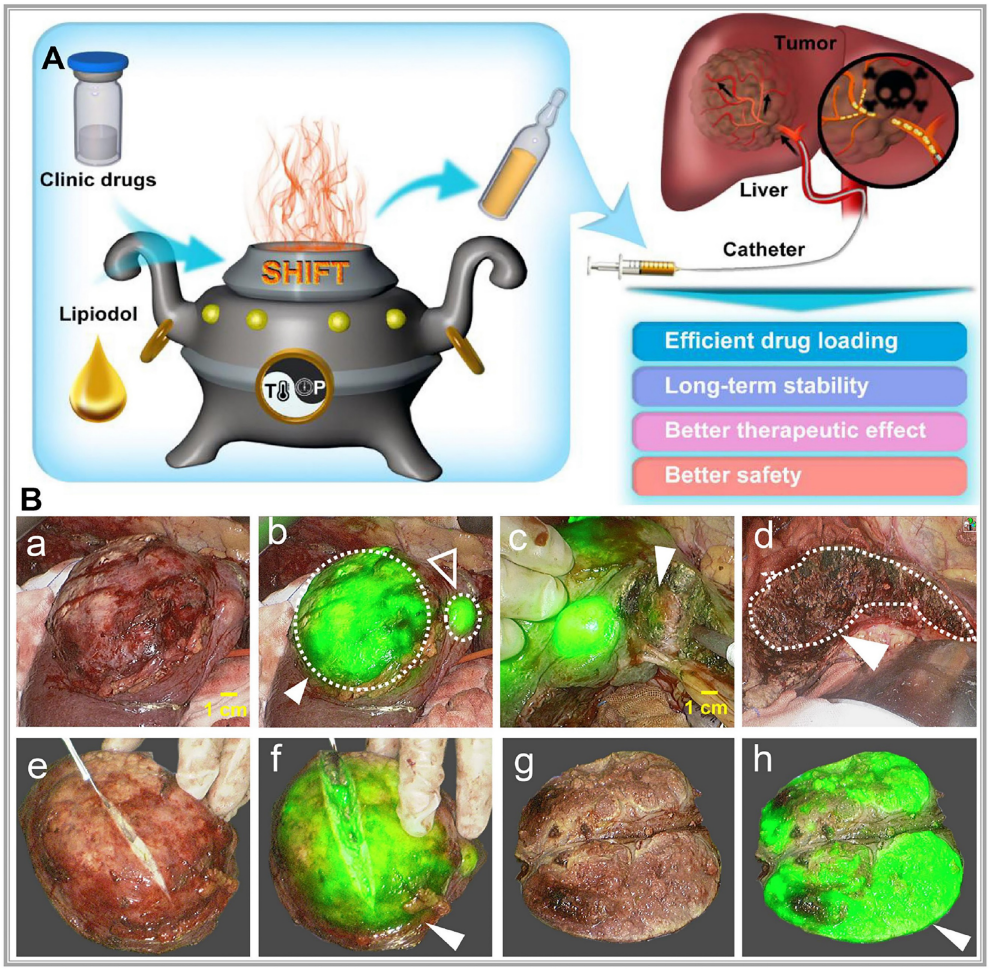

Figure 5. (A) Schematic illustration of superstable homogeneous intermixed formulation technology (SHIFT) as a revolutionary strategy for transhepatic arterial chem otherapy and embolization (TACE). Reproduced with permission from [59], copyright 2020, Elsevier. **(B)** The clinic drugs and lipiodol are introduced to develop formulations with SHIFT at a controlled temperature and pressure overcoming current challenges in the liver cancer treatment with TACE. Reproduced with permission from [60], copyright 2022, Wiley.

The goal of optical imaging systems is to capture and accurately display optical signals carrying specific biological information. Broadly, these systems are categorized into two main types based on their detection purposes: microscopic fluorescence imaging devices and macroscopic fluorescence imaging devices. However, significant technical and functional differences existed among devices based on different detection needs. With observation fields in the micrometer to sub-millimeter range, microscopic imaging devices provide high sensitivity and resolution for detailed visualization of tissue structures [62]. Examples include multiphoton microscopes, single-photon microscopes, laser scanning confocal microscopes, spectral encoding endoscopes, fluorescence resonance energy transfer microscopes, and radiomolecular imaging devices. These are predominantly used for *in vitro* or *in vivo* microscopic analysis. Macroscopic fluorescence imaging devices, with observation fields typically in the centimeter to millimeter range, are designed for preclinical studies and clinical applications. Examples include fluorescence imaging and bioluminescence imaging devices, which use non-contact external detection or endoscopic detection for studies on small animals and humans. Compared to microscopic imaging devices, these have a simpler structure and are well-suited for clinical or and research purposes [63,64].

The origins of macroscopic fluorescence imaging date back to 1994, when Roger Y. Tsien improved green fluorescent protein technology. This breakthrough enabled the pairing of lasers with charge coupled device cameras, leading to the development of *in vivo* fluorescence imaging devices [65-67]. Since then, global research institutions have advanced *in vivo* optical imaging devices to meet the growing demands of scientific research and clinical applications. For instance, in 1998, Professor Contag at Stanford University, in collaboration with partners, co-founded Xenogen Corporation, which pioneered the IVIS imaging system—a widely used bioluminescence imaging platform. In 2004, Professor Ge Wang's research team at Virginia Tech successfully developed an optical-CT multimodal imaging system, advancing the precision and scope of imaging technology. In 2005, Novadaq Technologies' SPY™ system became the first FDA-approved fluorescence molecular imaging system. This system is widely used in vascular surgery and for assisting surgical outcomes in breast cancer procedures [68]. In 2009, the Molecular Imaging Research and Development Center at the Institute of Automation, Chinese Academy of Sciences developed an original bioluminescence imaging system with patents in both the U.S. and China. In 2019, Beijing Digital Precision Medical Technology Co., Ltd. expanded applications for intraoperative navigation, allowing real-time localization of small cancer lesions (< 5mm) [69]. By 2022, the real-time super-sensitive fluorescence imaging system developed by the Tsinghua-IDG/McGovern Brain Institute team developed a high-sensitivity fluorescence imaging system, pushing the boundaries of imaging quality beyond particle noise limits, enhancing fluorescence imaging for biological research and clinical applications [70]. As the concepts of minimally invasive and precision surgery keep on evolving, commercially approved imaging and navigation devices have become integral in surgical guidance. Common clinical imaging and navigation devices used for clinical diagnosis and treatment are presented in **Figure 6**.

Clinical application of optical molecular imaging technology

Applications of optical molecular imaging technology can be categorized into three primary areas: (1) *In vivo* functional molecular detection: This approach uses *ex vivo* two- or three-dimensional optical imaging devices to analyze molecular functions and quantify molecules in living tumor tissues or diseased areas. (2) Therapeutics: In this category, multimodal probes are introduced into the body to not only image tumor tissues optically but also deliver therapeutic agents. (3) Intraoperative precision navigation: Optical probes are injected into the body before surgery. Specific lasers from the imaging system stimulate the probes to emit detectable signals. These signals outline detailed morphological information of the lesion on-screen, aiding surgeons in performing highly accurate procedures. This application has gained widespread use, particularly in hepatobiliary surgery, as fluorescence imaging offers high sensitivity and specificity, making it a valuable tool in diagnosing and treating liver cancer [74]. Fluorescent probes can selectively bind to liver cancer cells or specific molecules in the tumor microenvironment, emitting fluorescence signals that allow visualization of the cancerous areas. This method helps doctors identify the location and quantity of cancerous lesions with higher precision. It also provides real-time guidance for lesion removal during surgery, enhancing the accuracy and completeness of the resection [75]. These advancements significantly reduce the risk of postoperative recurrence and improve long-term survival rates for liver cancer patients.

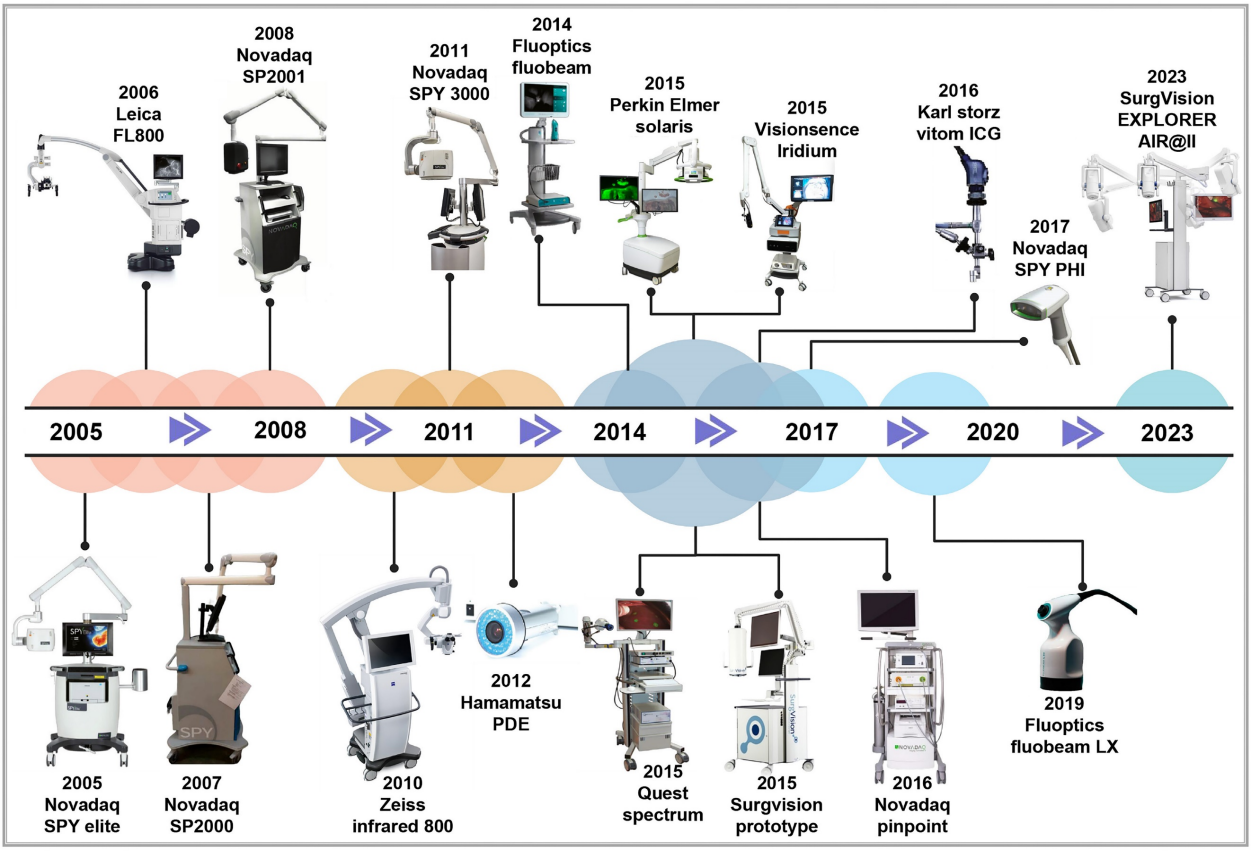

Figure 6. The developmental history of FDA-approved near-infrared fluorescence imaging and navigation systems. Reproduced with permission from [71-73]. This figure was created with Biorender.com.

Despite these advancements, the effectiveness of fluorescence imaging for liver cancer depends on stable and reliable fluorescence probes. Currently, available surgical navigation probes for liver cancer are limited, with intraoperative navigation primarily relying on ICG. However, ICG's low specificity and limited tissue penetration present challenges. Ideally, fluorescence probes for liver cancer imaging should have the following features: (1) ability to detect low concentrations of target molecules, enabling precise high-sensitivity imaging; (2) high spatial resolution to reveal minute biological and intracellular structures; (3) real-time imaging capabilities to capture dynamic changes during biological processes and complex surgical procedures; and (4) availability of various probe types to address different surgical requirements [76].

Research into near-infrared fluorescence probes is expanding, especially within the scope of liver cancer imaging. Current techniques primarily focus on imaging in two regions: near-infrared region I (NIR-I) and near-infrared region II (NIR-II). Each region offers unique imaging characteristics that contribute to liver cancer detection and treatment.

NIR-I fluorescence imaging

NIR-I spanning 700–900 nm, has unique properties that make it highly suitable for biological imaging, especially in clinical settings. NIR-I's deep tissue penetration and favorable optical characteristics make it ideal for cancer surgery navigation, molecular imaging, and analytical chemistry applications [77,78]. Several NIR fluorescence probes have been designed within this range to detect specific molecular biomarkers in tissues, cells, and molecules. These probes target diverse biomarkers, including enzymes, nitro compounds, thiols, metal ions, reactive oxygen species, and peptides, and are used in both biomedical and chemical analysis [79-81]. Existing NIR-I probes can be broadly classified into three categories, as shown in **Table 1**. Currently, approximately 30 NIR-I probes are clinically available [82], with FDA-approved probes such as ICG, methylene blue, and pafolacianine being the most commonly used. Among them, ICG is frequently employed in fluorescence-guided surgeries, particularly for liver cancer resection.

ICG is a water-soluble dye that binds tightly to plasma proteins, such as albumin when injected

intravenously. It is primarily cleared from the plasma by hepatocytes and excreted into the bile, eventually reaching the intestine (**Figure 7A**). Notably, ICG does not undergo metabolic changes during this process not participate in enterohepatic circulation (**Figure 7B**) [99]. Therefore, the rate of ICG clearance from the blood to the bile duct directly serves as a direct indicator of liver reserve function [100]. Specifically, the ICG 15-min blood retention rate has been well-recognized globally, particularly in the frequent use of preoperative liver functional reserve assessment [101,102]. Meanwhile, when exposed to light in the 750–810 nm range, ICG emits light at around 830 nm within the NIR-I range [103]. In the biological body, because of the scattering and absorption effects of hemoglobin and water molecules, light's penetration ability rapidly decreases. Hemoglobin absorbs strongly below 700 nm, while water is essentially transparent to visible and near-infrared light but strongly absorbs light above 900 nm. Thus, light in the NIR-I range (700–900 nm) achieves optimal penetration in biological tissues [104]. Due to these properties, ICG fluorescence can be detected as deep as approximately 10 mm beneath the tissue surface. Accordingly, ICG has been widely used in clinical applications for over 50 years. Although rare, mild allergic reactions are occasionally reported in patients due to the iodine content in ICG during long-term use [105].

Table 1. The classification of common NIR-I probe

Category	Chemical construction	Ref.
Small molecule fluorophore	Cyanines	[83]
	Porphyrin-based	[84]
	Mental complexes	[85]
	Xanthene dyes	[86, 87]
	Squaraine	[88, 89]
	Phenothiazine-based	[90]
	Bodipy	[91, 92]
	Dicyanomethylene–4H–pyran	[93]
Synthetic nanoparticles	Single walled carbon nanotubes	[94]
	Quantum dots	[95]
	Rare earth nanomaterials	[96]
Biologics	Near-infrared fluorescent proteins	[97]
	Phytochrome	[98]

The use of ICG for NIR-I imaging in liver cancer was pioneered in 2009 by Professor Ishizawa in Japan who performed real-time NIR-I imaging during surgeries on 63 liver cancer patients to delineate tumor boundaries. In eight of these cases, fluorescence-guided imaging revealed small, previously undetected lesions [106]. In 2014, Sakoda further advanced the approach by using ICG-guided NIR-I imaging to determine tumor boundaries, performing resections solely based on these imaging results with no adverse outcomes in patients [107]. Recent meta-analyses have also confirmed that ICG fluorescence NIR-I imaging effectively improves clinical outcomes in liver cancer surgeries [108-110]. With the widespread use of ICG NIR-I fluorescence

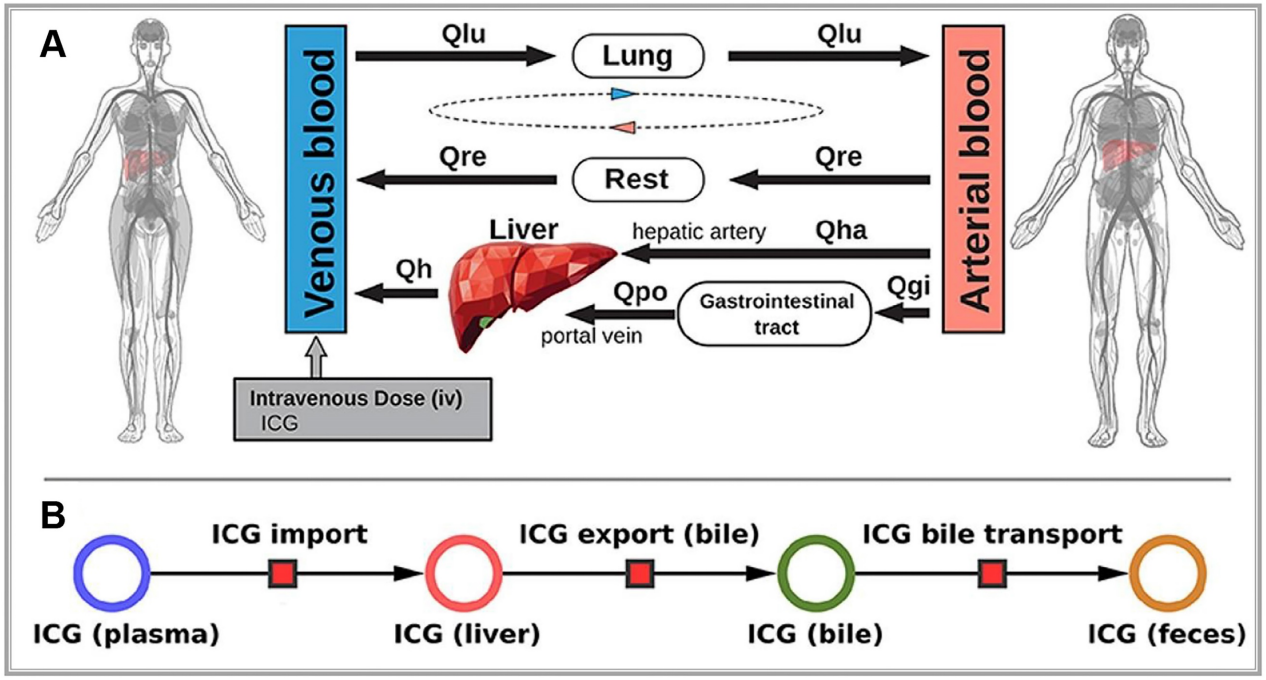

Figure 7. (A) Whole-body model: The whole-body PBPK model for ICG consists of venous blood, arterial blood, lung, liver, gastrointestinal tract, and rest compartment (accounting for organs not modeled in detail) and the systemic blood circulation connecting these compartments. **(B)** Liver model: ICG in the liver plasma compartment is taken up into the liver tissue (hepatocytes). Subsequently hepatic ICG is excreted in the bile from where it is excreted in the feces. No metabolization of ICG takes place in the liver. Reproduced with permission from [99], copyright 2021, Frontiers Media S.A.

imaging, ICG administration methods have been more meticulously studied, refining ICG dosage and timing protocols. For instance, Wakabayashi analyzed 72 relevant articles and concluded that for negative staining (detection of non-fluorescent tissues), a dose of 2.5 mg is optimal. By contrast, for positive staining (fluorescent tissue detection), a dose of 0.25 mg per patient is recommended [111]. Such findings provide a theoretical basis for standardizing ICG use in clinical settings.

Furthermore, in addition to high-performance imaging probes, imaging devices are essential for achieving excellent performance in NIR-I imaging. Beyond probe technology, the development of high-performance NIR-I imaging devices has also matured, focusing currently on improving instruments by enhancing operational convenience and refining data processing capabilities. For example, the novel "Click-on" fluorescence detector developed by Oosterom [112] converts robotic surgical tools into molecular sensors, allowing surgeons to detect NIR signals under standard white light conditions. In a pig model, this technology was successfully tested for surgical applications such as vascular imaging and lymphatic mapping. Regarding data refining, Azargoshasb [113] demonstrated an innovative approach to improve fluorescence-guided surgery by tracking the real-time positions of surgical instruments. By converting positional data into dynamic digital information, they calculated the relationship between instrument position and signal-to-background ratio (SBR) to quantify the impact of SBR on fluorescence-guided surgery conducted for lesion discrimination. Results revealed that when SBR fell below 1.5, differentiating reflected excitation light from low-intensity fluorescence emission signals became difficult, increasing the risk of surgical errors. Therefore, by combining SBR quantification with kinematic scoring, this approach provides an enhanced framework for precision in fluorescence-guided surgery in clinical practice.

NIR-II fluorescence imaging

Compared with NIR-I imaging, fluorescent probes in the NIR-II range emit fluorescence signals in the range of approximately 1000–1700 nm [114]. This spectral window is further divided into subregions, including NIR-IIa' (1000–1300 nm), NIR-IIa (1300–1400 nm), and NIR-IIb (1500–1700 nm) [77]. While NIR-I imaging offers substantial improvements over visible light wavelengths, emerging research suggests that NIR-II imaging further enhances image quality in live subjects. The key advantages of NIR-II imaging are as follows [61,78]: (1) Higher tissue penetration depth: NIR-II wavelengths penetrate biological tissues more effectively than NIR-I, achieving depths up to 3 cm and reducing interference from tissue scattering and absorption; (2) Strong anti-interference capability: Biological tissues produce minimal background fluorescence within the NIR-II range, resulting in higher image contrast and improved detection of fluorescence signals; and (3) Higher image resolution: NIR-II fluorescence enables detailed, high-resolution imaging at the cellular level, making it highly relevant for clinical applications.

NIR-II *in vivo* macroscopic imaging systems are particularly useful in basic research for visualizing entire organisms or specific organs in animal models, such as mice, rats, rabbits, and monkeys. In clinical applications, NIR-II imaging assists with real-time surgical navigation, intraoperative precise imaging, and macroscopic biopsy guidance [115]. NIR-II microscopic systems enable detailed structural analysis at the micro-level. Additionally, the development of NIR-II fluorescence endoscopy is advancing minimally invasive laparoscopic surgeries. Currently, clinical translation of advanced medical imaging devices, including NIR-II macroscopic, microscopic, and endoscopic systems, is now a major research focus.

A wide array of NIR-II probes is currently available, including organic fluorophores, single-walled carbon nanotubes, quantum dots, and rare-earth nanoparticles [116-118]. However, these probes are mostly restricted to preclinical research. Among clinically approved NIR probes, fortunately, ICG is widely used as it emits light up to 1200 nm, extending partially into the NIR-II range, thus offering a pathway for the clinical application of NIR-II fluorescence imaging [119,120]. Moreover, ICG exhibits a higher quantum yield within the NIR-II range, making it a practical candidate for clinical applications in NIR-II imaging [121]. Based on this, Starosolski speculated that through interactions with lipid molecules, organic media, and plasma, ICG may exhibit enhanced NIR-II signal performance, providing potential pathways for optimizing its clinical use [122].

Recent technological advances have also led to the development of more cost-effective NIR-II imaging devices by using compound semiconductor detectors made from InGaAs or HgCdTe, which capture high-sensitivity, high-contrast images in the NIR-II range [123]. Multiple research teams are developing NIR-II imaging devices for practical clinical applications. For instance, a multispectral fluorescence imaging device developed by our research team, covering the spectral range of 400–1700 nm and enabling the simultaneous use of visible, NIR-I, and NIR-II imaging (**Figure 8**) [115]. Using this

device, they successfully conducted the first liver tumor surgery guided by multispectral fluorescence imaging, comparing tumor visibility across NIR-I and NIR-II imaging methods. This study, conducted on 23 liver cancer patients who received ICG injections, found that the tumor-to-normal-tissue ratio was higher in the NIR-II group than in the NIR-I group, both inside and outside the liver. Moreover, NIR-II imaging could detect tumor lesions that NIR-I imaging could not. The performance of NIR-II imaging in tumor identification was superior to that of NIR-I imaging. Wu constructed a portable NIR-II imaging system covering the 900–1700 nm spectral range [124]. In this system, ICG was used for the first time in microsurgery navigation. The system assessed vascular patency during vessel anastomosis, arterial blood supply and venous drainage during finger replantation, and skin perforator vessels and skin flap perfusion. NIR-II imaging was found to be less affected by interfering factors than NIR-I imaging, resulting in clearer images and higher contrast, which effectively improved the accuracy of decision-making in surgical procedures.

Furthermore, in addition to hepatobiliary surgery, ICG-based NIR-II imaging has been applied in various fields. For example, Li precisely detected pancreatic cancer by using ICG-assisted NIR-I and NIR-II window fluorescence imaging techniques [125]. Cao first used ICG-based NIR-II imaging for fluorescence-guided surgery in nephrectomy, with no tumor recurrence or metastasis noted in nine postoperative patients [126]. In a randomized controlled trial, after conducting guided surgical resection for 33 patients with high-grade gliomas, Shi found a 100% complete resection rate in 15 patients guided by ICG-based NIR-II imaging [127]. Furthermore, Shen combined *in situ* ICG NIR-II imaging with deep convolutional neural networks for pathological glioma diagnosis in real time. This approach was more sensitive than the experiential judgment of doctors (96.8% vs. 82%), which enables rapid intraoperative prediction of tumor malignancy grading and Ki-67 levels [128]. This study provides robust support for the widespread clinical use of ICG's NIR-II imaging. Considering ICG is extensively used in various diagnostic and therapeutic scenarios, this technology may have broader prospects in clinical settings.

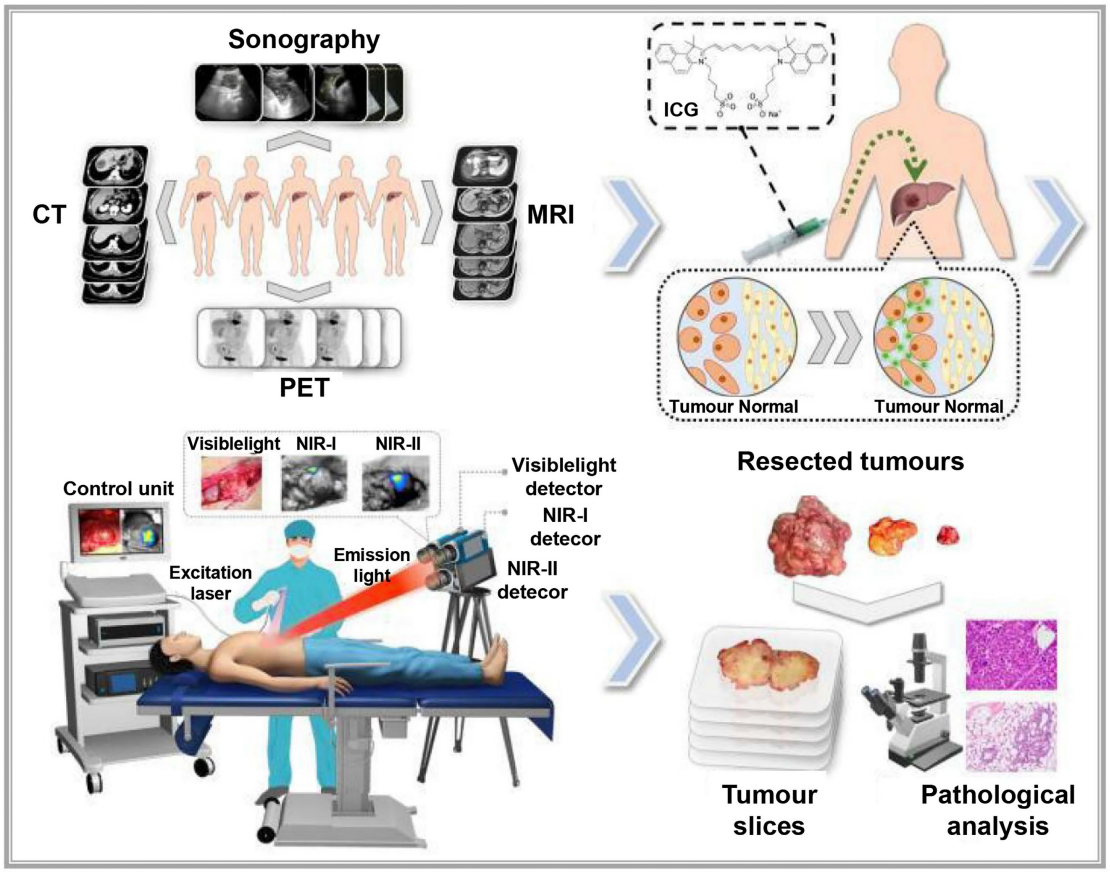

Figure 8. Description of the study plan and the visible and NIR-I/II multispectral imaging instrument for clinical applications: Patients with liver cancer were enroled in the study, and then received preoperative imaging examinations, including enhanced CT, MRI, ultrasonography and PET. Before surgery, the patients were injected with ICG intravenously at a dose of 0.5 mg/kg body weight as a routine preoperative liver function test. One to seven days later, on the day of surgery, the patients received a laparotomy. The liver surface was examined by the integrated NIR-I/II and visible multispectral imaging instrument and visible and NIR-I/II images were obtained. Tumors were resected by the guidance of ultrasonography and NIR-I imaging. During the resection, NIR-II images were also acquired. After the operation, visible and NIR-I/II images of the resected specimens were obtained. Pathological examination of the resected tissues was conducted. Reproduced with permission from [115], copyright 2022, Springer Nature.

The new integrated model of interventional molecular imaging

In clinical diagnosis and treatment, late-stage liver cancer is often marked by subtle, invasive growth patterns that typically remain undetected until advanced stages. This progression is frequently accompanied by multiple microsatellite and metastatic foci, which can hinder early intervention efforts [129]. Interventional embolization can offer a chance for surgical resection by converting otherwise inoperable cases into surgically manageable ones [130]. However, even with the chance for surgical resection after interventional embolization, intraoperatively, unclear tumor tissue boundaries and hidden microlesions may not be completely and thoroughly removed, leading to a high postoperative recurrence rate. Traditional ICG-based fluorescence navigation, though helpful for identifying liver tumors, falls short in cases where embolization hinders arterial blood flow and induces cancer necrosis. These changes disrupt ICG distribution within the tumor, limiting its effectiveness for precise surgical navigation in embolization-treated liver cancer cases [131]. Developing interventional molecular imaging technology, therefore, remains essential to improve therapeutic outcomes for late-stage liver cancer.

Currently, clinical research on interventional molecular imaging is limited, with the most representative work involving intraoperative segmental staining of liver cancer by injecting ICG via the ultrasound-guided portal vein or, preoperatively, through the microcatheter super-selective tumor-feeding artery under digital subtraction angiography guidance, which allows for precise fluorescence-guided surgical resection. For example, Xu successfully performed high-precision laparoscopic anatomical liver resection by injecting 5–10 mL of ICG (0.025 mg/mL) into tumor-feeding portal vein branches under intraoperative ultrasound guidance, thus primarily achieving positive staining [132]. According to Li *et al.*, fluorescence-positive staining of liver segments can be achieved in laparoscopic liver cancer surgery by superselectively administering ICG through the arteries, thereby evaluating its effectiveness [133]. However, the aforementioned methods, which use interventional approaches to achieve precise ICG fluorescence imaging, only address the method of ICG injection and not the drawbacks of ICG, such as its rapid metabolism as a small molecule drug, local diffusion, and fluorescence quenching. Importantly, effective approaches for implementing fluorescence navigation after liver cancer embolization are not available.

Combining interventional embolic agents with fluorescent molecular dyes is promising in addressing the downstaging of advanced liver cancer while enabling fluorescence-guided surgical diagnosis and treatment. However, developing an ideal fluorescent-labeled embolic agent requires overcoming two main challenges: achieving a uniform fluorescent dye dispersion within the embolic agent and maintaining the dye's stability for an extended period, ensuring that the fluorescence optical properties of the dye remain unaffected. To address these issues, our team developed a super-stable homogenization technique that creates a stable, uniformly mixed formulation of clinical lipiodol embolic agents with ICG, known as SHIFT&ICG. This novel formulation is being rapidly applied in the downstaging and fluorescence-guided resection of advanced liver cancer [134]. In a clinical retrospective study, the SHIFT&ICG formulation prepared using this technique exhibited excellent tumor deposition efficacy and safety. During surgical resection after long-term conversion therapy for liver cancer, facilitating real-time visualization of tumor areas and boundaries, which ensures complete removal of primary lesions and tiny metastatic foci. This approach improves surgical precision while minimizing complications related to surgery, anesthesia, and postoperative recovery. SHIFT&ICG thus provides a new approach for improving the accuracy of liver cancer resection after interventional embolization therapy [131].

Moreover, to further enhance fluorescence imaging performance, our team has developed a pure drug nanoparticle technology. This method nano-sizes ICG without altering its molecular structure, resulting in a formulation called SHIFT&nanoICG, which resists photobleaching and exhibits superior fluorescence imaging performance compared to conventional ICG formulations. The challenges associated with traditional ICG formulations, such as rapid decay and lower resolution, have been effectively addressed by SHIFT&nanoICG [130], which has been validated through clinical experiments. This formulation can enable accurate fluorescence navigation for microsatellite lesions that often go undetected in preoperative imaging [135]. With its significant translational potential, SHIFT&nanoICG is set to redefine interventional embolization techniques for fluorescence-guided liver cancer surgery, paving the way for a more effective surgical model, the research process is shown in **Figure 9A-D.**

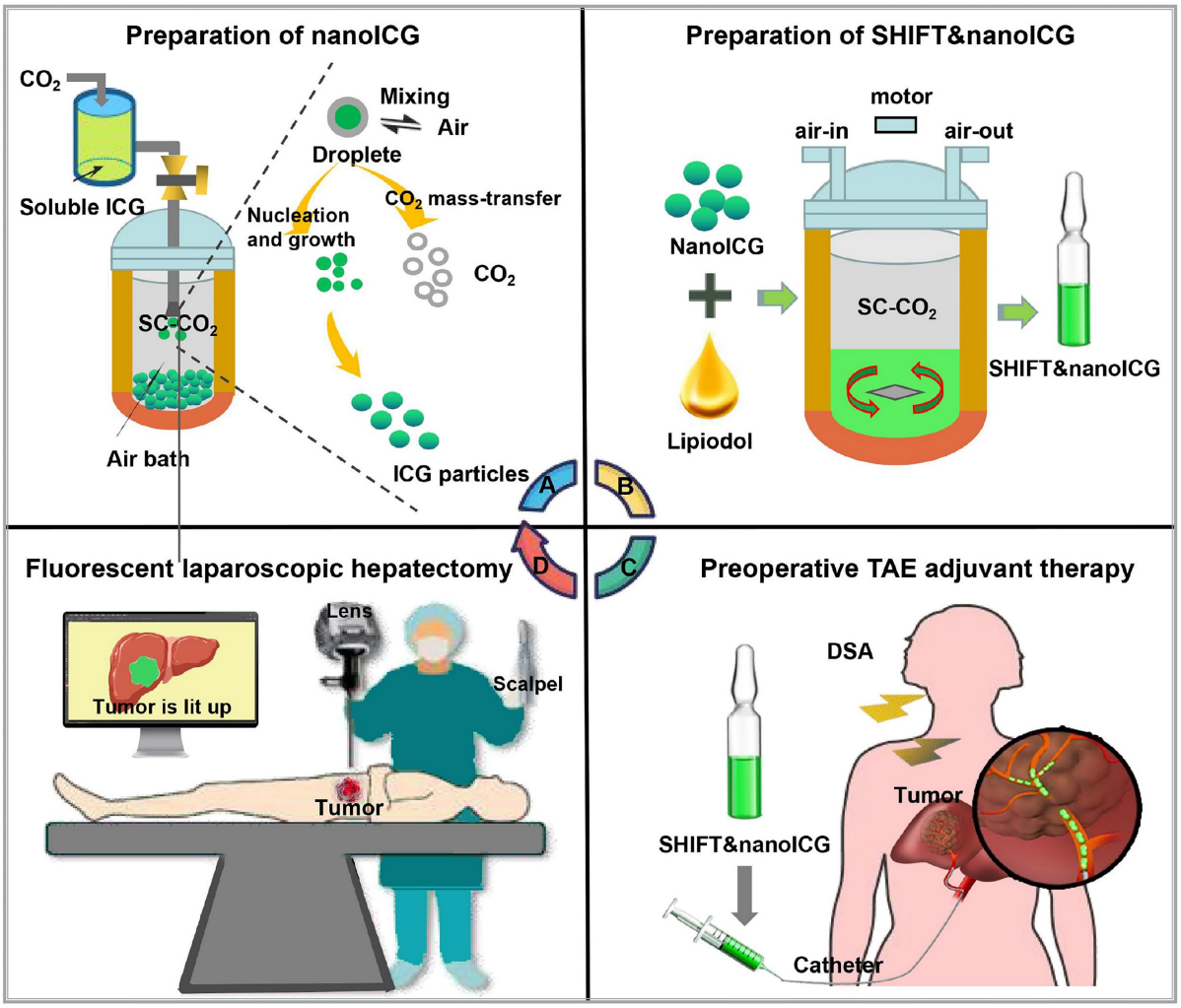

Figure 9. (A) Supercritical anti-solvent process was employed to produce carrier-free nanoICG withenhanced imaging properties and anti-photobleaching capacity. **(B)** Superstable homogeneous intermixed formulation technology (SHIFT) wasemployed to produce SHIFT&nanoICG for theranostics. **(C)** Preoperative transcatheterarterial embolization (TAE) adjuvant therapy with SHIFT&nanoICG as the embolic agent. **(D)** Thepatient received a precise laparoscopic hepatectomy under real-time fuorescence after TAE. DSA, digital subtraction angiography; SC-CO2, supercritical carbon dioxide. Reproduced with permission from [135], copyright 2022, BioMed Central.

Summary and prospect

The future development of NIR imaging technology in precision medicine promises to advance individualized and customized surgical solutions to patients' specific needs. For example, by integrating fluorescence navigation with other imaging modalities, clinicians may achieve enhanced detection of liver cancer and its metastatic foci, including improved assessment of tumor depth [136]. Although optical molecular imaging, primarily NIR-II imaging, has been tested in various disease models, clinical research remains scarce, with few multicenter, large-sample studies providing prospective data. Simultaneously, the optimization and miniaturization of detection devices will be essential to support broader applications in surgical practice.

Looking ahead, optical molecular imaging is poised to play an increasingly significant role in liver cancer treatment. On one hand, with ongoing advancements, the technology's resolution and sensitivity will improve, allowing medical professionals to more accurately locate and identify tiny tumor lesions. On the other hand, incorporating machine learning and artificial intelligence will make molecular imaging more intelligent, supporting surgical decision-making, reducing surgical errors, and improving the success and accuracy of surgical procedures. Additionally, this technology will also be vital in postoperative follow-up, enabling clinicians to monitor recovery, track tumor recurrence, and adapt treatment plans promptly, thereby improving patients' overall survival rates and quality of life.

In biomedical research and clinical practice, any single detection method is associated with limitations. Integrating fluorescence imaging with other advanced diagnostic imaging methods or other therapeutic approaches, such as targeted therapy, and immunotherapy, is promising for further enhancing the therapeutic outcomes of liver cancer surgery.

Through comprehensive treatment strategies, fluorescence imaging technology may offer more personalized and precise treatment plans for liver cancer patients [137]. Although optical molecular imaging shows potential in clinical trials, transitioning these findings into routine practice presents challenges. This will require interdisciplinary collaboration, with involvement from physicians, biologists, and engineers, alongside rigorous clinical trials and regulatory approval processes. Before further clinical development, several factors must be addressed for successful clinical translation: (1) the combination of imaging agents with carriers or ligands may alter the pharmacokinetics and biodistribution of fluorescent dyes, potentially introducing new side effects; (2) mitigating the toxicity of complex probe structures is critical, especially given risks such as cardiotoxicity, renal and hepatic impairment, and neurotoxicity. Modifying the preparation techniques of imaging probes, optimizing the materials used, and selecting appropriate administration routes may provide references for addressing these issues. Developing imaging probes through carrier-free methods, such as Liu's pure drug nanotechnology, which avoids organic solvents and toxic chemicals, could help tackle these issues. Additionally, choosing clinically approved drugs or their components as raw materials for optical probes or optimizing administration routes may minimize side effects, simplify the manufacturing process, and expedite clinical application.

In conclusion, optical molecular imaging offers a promising future in precise liver cancer surgical navigation. However, realizing its full potential will require ongoing innovation and interdisciplinary collaboration. With continued advancements and extensive clinical research, fluorescence imaging technology centered on optical molecular imaging is expected to become integral to liver cancer treatment, supporting more effective, personalized, and life-enhancing outcomes.

Acknowledgements

This work was supported by the National Natural Science Foundation of China (82302403, 82373189, 8237202, 81925019), the National Key Research and Development Program of China (2023YFB3810000, 2023YFC241570), the Key Program of the Joint Fund of the National Natural Science Foundation of China (U24A20746, U24A20525), the Unveiling and Leading Projects of Affiliated Hospital of North Sichuan Medical College (2022JB003), Nanchong science and technology plan project 23JCYJPT0043.

Author contributions

G. L., P. H., and Y. Z. (Yu Zhang) conceived and revised the paper. P. H., and H. T. drafted the manuscript and prepared the figures and tables. Y. Z., X. X., T. J., X. P., Y. X., and Y. Z. (Yang Zhang) are responsible for part of the data collection. All authors read and approved the final manuscript.

Competing Interests

The authors have declared that no competing interest exists.

References

1. Zhang J, Rector J, Lin JQ, Young JH, Sans M, Katta N, et al. Nondestructive tissue analysis for *ex vivo* and *in vivo* cancer diagnosis using a handheld mass spectrometry system. Sci Transl Med. 2017; 9: eaan3968.
2. Niu G, Chen X. Lymphatic imaging: focus on imaging probes. Theranostics. 2015; 5: 686-97.
3. Xia Y, Zhang R, Wang Z, Tian J, Chen X. Recent advances in high-performance fluorescent and bioluminescent RNA imaging probes. Chem Soc Rev. 2017; 46: 2824-2843.
4. Weissleder R. Scaling down imaging: molecular mapping of cancer in mice. Nat Rev Cancer. 2002; 2: 11-18.
5. Lim EA, Drake CG, Mintz A. Molecular imaging for cancer immunotherapy. Immunooncol Technol. 2020; 5: 10-21.
6. Mondal SB, O'Brien CM, Bishop K, Fields RC, Margenthaler JA, Achilefu S. Repurposing molecular imaging and sensing for cancer image-guided surgery. J Nucl Med. 2020; 61: 1113-1122.
7. Youn H, Hong KJ. *In vivo* noninvasive molecular imaging for immune cell tracking in small animals. Immune Netw. 2012; 12: 223-9.
8. Kelloff GJ, Krohn KA, Larson SM, Weissleder R, Mankoff DA, Hoffman JM, et al. The progress and promise of molecular imaging probes in oncologic drug development. Clin Cancer Res. 2005; 11: 7967-85.
9. Weissleder R, Mahmood U. Molecular imaging. Radiology. 2001; 219: 316-333.
10. Chaturvedi S, Kaul A, Hazari PP, Mishra AK. Mapping neuroreceptors with metal-labeled radiopharmaceuticals. Medchemcomm. 2017; 8: 855-870.
11. Hernot S, van Manen L, Debie P, Mieog JSD, Vahrmeijer AL. Latest developments in molecular tracers for fluorescence image-guided cancer surgery. Lancet Oncol. 2019; 20: e354-e367.
12. Herschman HR. Molecular imaging: looking at problems, seeing solutions. Science. 2003; 302: 605-8.
13. Jaffer FA, Weissleder R. Molecular imaging in the clinical arena. JAMA. 2005; 293: 855-62.
14. Rao J, Dragulescu-Andrasi A, Yao H. Fluorescence imaging *in vivo*: recent advances. Curr Opin Biotechnol. 2007; 18: 17-25.
15. Dehkharghanian T, Hashemiaghdam A, Ashrafi G. Semiautomated analysis of an optical ATP indicator in neurons. Neurophotonics. 2022; 9: 041410.
16. Munch M, Rotstein BH, Ulrich G. Fluorine-18-labeled fluorescent dyes for dual-mode molecular imaging. Molecules. 2020; 25: 6042.
17. Zhao Y, Tietz O, Kuan WL, Haji-Dheere AK, Thompson S, Vallin B, et al. A fluorescent molecular imaging probe with selectivity for soluble tau aggregated protein. Chem Sci. 2020; 11: 4773-4778.
18. rapiella-Alfonso L, Pons T, Lequeux N, Leleu L, Grimaldi J, Tasso M, et al. Clickable-zwitterionic copolymer capped-quantum dots for *in vivo* fluorescence tumor imaging. ACS Appl Mater Interfaces. 2018; 10: 17107-17116.
19. Refaat A, Yap ML, Pietersz G, Walsh APG, Zeller J, Del Rosal B, et al. *In vivo* fluorescence imaging: success in preclinical imaging paves the way for clinical applications. J Nanobiotechnology. 2022; 20: 450.
20. Mieog JSD, Achterberg FB, Zlitni A, Hutteman M, Burggraaf J, Swijnenburg RJ, et al. Fundamentals and developments in fluorescence-guided cancer surgery. Nat Rev Clin Oncol. 2021; 19: 9-22.
21. Frangioni JV. *In vivo* near-infrared fluorescence imaging. Curr Opin Chem Biol. 2003; 7: 626-634.
22. Sakka SG, van Hout N. Relation between indocyanine green (ICG) plasma disappearance rate and ICG blood clearance in critically ill patients. Intensive Care Med. 2006; 32: 766-769.
23. Segal E, Satchi-Fainaro R. Design and development of polymer conjugates as anti-angiogenic agents. Adv Drug Deliv Rev. 2009; 61: 1159-1176.
24. Yu M, Zheng J. Clearance pathways and tumor targeting of imaging nanoparticles. ACS Nano. 2015; 9: 6655-6674.
25. Benson RC, Kues HA. Fluorescence properties of indocyanine green as related to angiography. Phys Med Biol. 1978; 23: 159-63.
26. Wang X, Teh CSC, Ishizawa T, Aoki T, Cavallucci D, Lee SY, et al. Consensus guidelines for the use of fluorescence imaging in hepatobiliary surgery. Ann Surg. 2021; 274: 97-106.

27. Sindhwani S, Syed AM, Ngai J, Kingston BR, Maiorino L, Rothschild J, et al. The entry of nanoparticles into solid tumours. Nat Mater. 2020; 19: 566-575.
28. Wang Q, Liang Q, Dou J, Zhou H, Zeng C, Pan H, et al. Breaking through the basement membrane barrier to improve nanotherapeutic delivery to tumours. Nat Nanotechnol. 2024; 19: 95-105.
29. Vahrmeijer AL, Hutteman M, van der Vorst JR, van de Velde CJ, Frangioni JV. Image-guided cancer surgery using near-infrared fluorescence. Nat Rev Clin Oncol. 2013; 10: 507-518.
30. Favril S, Abma E, Blasi F, Stock E, Devriendt N, Vanderperren K, et al. Clinical use of organic near-infrared fluorescent contrast agents in image-guided oncologic procedures and its potential in veterinary oncology. Vet Rec. 2018; 183: 354.
31. Folli S, Westermann P, Braichotte D, Pèlegrin A, Wagnières G, van den Bergh H, et al. Antibody-indocyanin conjugates for immunophotodetection of human squamous cell carcinoma in nude mice. Cancer Res. 1994; 54: 2643-2649.
32. Ntziachristos V. Fluorescence molecular imaging. Annu Rev Biomed Eng. 2006; 8: 1-33.
33. Wenk CH, Ponce F, Guillermet S, Tenaud C, Boturyn D, Dumy P, et al. Near-infrared optical guided surgery of highly infiltrative fibrosarcomas in cats using an anti-αvß3 integrin molecular probe. Cancer Lett. 2013; 334: 188-195.
34. Bohrmann L, Burghardt T, Haynes C, Saatchi K, Häfeli UO. Aptamers used for molecular imaging and theranostics-recent developments. Theranostics. 2022; 12: 4010.
35. Park D, Don AS, Massamiri T, Karwa A, Warner B, MacDonald J, et al. Noninvasive imaging of cell death using an Hsp90 ligand. J Am Chem Soc. 2011; 133: 2832-2835.
36. Luo Q, Shao N, Zhang AC, Chen CF, Wang D, Luo LP, et al. Smart Biomimetic Nanozymes for Precise Molecular Imaging: Application and Challenges. Pharmaceuticals (Basel). 2023; 16: 249.
37. Hellebust A, Richards-Kortum R. Advances in molecular imaging: targeted optical contrast agents for cancer diagnostics. Nanomedicine. 2012; 7: 429-445.
38. Weissleder R, Tung CH, Mahmood U, Bogdanov A Jr. *In vivo* imaging of tumors with protease-activated near-infrared fluorescent probes. Nat Biotechnol. 1999; 17: 375-378.
39. Sahl SJ, Hell SW, Jakobs S. Fluorescence nanoscopy in cell biology. Nat Rev Mol Cell Biol. 2017; 18: 685-701.
40. Josserand V, Bernard C, Michy T, Guidetti M, Vollaire J, Coll JL, et al. Tumor-specific imaging with angiostamp800 or bevacizumab-IRDye 800CW improves fluorescence-guided surgery over indocyanine green in peritoneal carcinomatosis. Biomedicines. 2022; 10: 1059.
41. Swamy MMM, Murai Y, Monde K, Tsuboi S, Jin T. Shortwave-infrared fluorescent molecular imaging probes based on π-conjugation extended indocyanine green. Bioconjug Chem. 2021; 32: 1541-1547.
42. Shi H, Huttad LV, Tan M, Liu H, Chua MS, Cheng Z, et al. NIR-II imaging of hepatocellular carcinoma based on a humanized anti-GPC3 antibody. RSC Med Chem. 2021; 13: 90-97.
43. Kobayashi H, Choyke PL. Target-cancer-cell-specific activatable fluorescence imaging probes: rational design and *in vivo* applications. Acc Chem Res. 2011; 44: 83-90.
44. Duan QJ, Zhao ZY, Zhang YJ, Fu L, Yuan YY, Du JZ, et al. Activatable fluorescent probes for real-time imaging-guided tumor therapy. Adv Drug Deliv Rev. 2023; 196: 114793.
45. Takahashi R, Ishizawa T, Sato M, Inagaki Y, Takanka M, Kuriki Y, et al. Fluorescence imaging using enzyme-activatable probes for real-time identification of pancreatic cancer. Front Oncol. 2021; 11: 714527.
46. Zeng Z, Liew SS, Wei X, Pu K. Hemicyanine-based near-infrared activatable probes for imaging and diagnosis of diseases. Angew Chem Int Ed Engl. 2021; 60: 26454-26475.
47. Li H, Kim D, Yao Q, Ge H, Chung J, Fan J, et al. Activity-based NIR enzyme fluorescent probes for the diagnosis of tumors and image-guided surgery. Angew Chem Int Ed Engl. 2021; 60: 17268-17289.
48. Zhao Z, Swartchick CB, Chan J. Targeted contrast agents and activatable probes for photoacoustic imaging of cancer. Chem Soc Rev. 2022; 51: 829-868.
49. Liu J, Siegmund KD. An evaluation of processing methods for HumanMethylation450 BeadChip data. BMC Genomics. 2016; 17: 469.
50. Ogawa M, Kosaka N, Choyke PL, Kobayashi H. *In vivo* molecular imaging of cancer with a quenching near-infrared fluorescent probe using conjugates of monoclonal antibodies and indocyanine green. Cancer Res. 2009; 69: 1268-72.
51. Yan R, Hu Y, Liu F, Wei S, Fang D, Shuhendler AJ, e al. Activatable NIR fluorescence/MRI bimodal probes for *in vivo* imaging by enzyme-mediated fluorogenic reaction and self-assembly. J Am Chem Soc. 2019; 141: 10331-10341.
52. Yan H, Gao X, Zhang Y, Chang W, Li J, Li X, et al. Imaging tiny hepatic tumor xenografts via endoglin-targeted paramagnetic/optical nanoprobe. ACS Appl Mater Interfaces. 2018; 10: 17047-17057.
53. Yeh CS, Su CH, Ho WY, Huang CC, Chang JC, Chien YH, et al. Tumor targeting and MR imaging with lipophilic cyanine-mediated near-infrared responsive porous Gd silicate nanoparticles. Biomaterials. 2013; 34: 5677-5688.
54. Chen Q, Liang C, Wang X, He J, Li Y, Liu Z. An albumin-based theranostic nano-agent for dual-modal imaging guided photothermal therapy to inhibit lymphatic metastasis of cancer post surgery. Biomaterials. 2014; 35: 9355-9362.
55. Shi S, Chen F, Goel S, Graves SA, Luo H, Theuer CP, et al. *In vivo* tumor-targeted dual-modality PET/optical imaging with a yolk/shell-structured silica nanosystem. Nanomicro Lett. 2018; 10: 65.
56. Lütje S, Rijpkema M, Goldenberg DM, van Rij CM, Sharkey RM, McBride WJ, et al. Pretargeted dual-modality immuno-SPECT and near-infrared fluorescence imaging for image-guided surgery of prostate cancer. Cancer Res. 2014; 74: 6216-6223.
57. Hekman MC, Rijpkema M, Muselaers CH, Oosterwijk E, Hulsbergen-Van de Kaa CA, Boerman OC, et al. Tumor-targeted dual-modality imaging to improve intraoperative visualization of clear cell renal cell carcinoma: a first in man study. Theranostics. 2018; 8: 2161.
58. Kang J, Chang JH, Kim SM, Lee HJ, Kim H, Wilson BC, et al. Real-time sentinel lymph node biopsy guidance using combined ultrasound, photoacoustic, fluorescence imaging: *in vivo* proof-of-principle and validation with nodal obstruction. Sci Rep. 2017; 7: 45008.
59. Cheng H, Yang X, Liu G. Superstable homogeneous iodinated formulation technology: revolutionizing transcatheter arterial chemoembolization. Sci Bull (Beijing). 2020; 65: 1685-1687.
60. He P, Xiong Y, Luo B, Liu J, Zhang Y, Xiong Y, et al. An exploratory human study of superstable homogeneous lipiodol-indocyanine green formulation for precise surgical navigation in liver cancer. Bioeng Transl Med. 2022; 8: e10404.
61. Zhang RR, Schroeder AB, Grudzinski JJ, Rosenthal EL, Warram JM, Pinchuk AN, et al. Beyond the margins: real-time detection of cancer using targeted fluorophores. Nat Rev Clin Oncol. 2017; 14: 347-364.
62. Choi HS, Kim HK. Multispectral image-guided surgery in patients. Nat Biomed Eng. 2020; 4: 245-246.
63. Lang P, Yeow K, Nichols A, Scheer A. Cellular imaging in drug discovery. Nat Rev Drug Discov. 2006; 5: 343-56.
64. Weissleder R, Pittet MJ. Imaging in the era of molecular oncology. Nature. 2008; 452: 580-589.
65. Pierce MC, Javier DJ, Richards-Kortum R. Optical contrast agents and imaging systems for detection and diagnosis of cancer. Int J Cancer. 2008; 123: 1979-1990.
66. Inouye S, Tsuji FI. Aequorea green fluorescent protein. FEBS Lett. 1994; 341: 277-280.
67. Heim R, Prasher DC, Tsien RY. Wavelength mutations and posttranslational autoxidation of green fluorescent protein. Proc Natl Acad Sci U S A. 1994; 91: 12501-12504.
68. Matz MV, Fradkov AF, Labas YA, Savitsky AP, Zaraisky AG, Markelov ML, et al. Fluorescent proteins from nonbioluminescent anthozoa species. Nat Biotechnol. 1999; 17: 969-973.
69. Munabi NC, Olorunnipa OB, Goltsman D, Rohde CH, Ascherman JA. The ability of intra-operative perfusion mapping with laser-assisted indocyanine green angiography to predict mastectomy flap necrosis in breast reconstruction: a prospective trial. J Plast Reconstr Aesthet Surg. 2014; 67: 449-455.
70. Zhang Z, He K, Chi C, Hu Z, Tian J. Intraoperative fluorescence molecular imaging accelerates the coming of precision surgery in China. Eur J Nucl Med Mol Imaging. 2022; 49: 2531-2543.
71. Li X, Li Y, Zhou Y, Wu J, Zhao Z, Fan J, et al. Real-time denoising enables high-sensitivity fluorescence time-lapse imaging beyond the shot-noise limit. Nat Biotechnol. 2023; 41: 282-292.
72. Sajedi S, Sabet H, Choi HS. Intraoperative biophotonic imaging systems for image-guided interventions. Nanophotonics. 2018; 8: 99-116.
73. DSouza AV, Lin H, Henderson ER, Samkoe KS, Pogue BW. Review of fluorescence guided surgery systems: identification of key performance capabilities beyond indocyanine green imaging. J Biomed Opt. 2016; 21: 80901.
74. Chi C, Du Y, Ye J, Kou D, Qiu J, Wang J, et al. Intraoperative imaging-guided cancer surgery: from current fluorescence molecular imaging methods to future multi-modality imaging technology. Theranostics. 2014; 4: 1072-84.
75. Shu Y, Huang C, Liu H, Hu F, Wen H, Liu J, et al. A hemicyanine-based fluorescent probe for simultaneous imaging of carboxylesterases and histone deacetylases in hepatocellular carcinoma. Spectrochim Acta A Mol Biomol Spectrosc. 2022; 281: 121529.
76. Han X, Xing Y, Song X, Dou K, Yu F, Chen L. Bioimaging of glutathione variation for early diagnosis of hepatocellular carcinoma using a liver-targeting ratiometric near-infrared fluorescent probe. J Mater Chem B. 2023; 11: 6612-6620.
77. Zhao J, Chen J, Ma S, Liu Q, Huang L, Chen X, et al. Recent developments in multimodality fluorescence imaging probes. Acta Pharm Sin B. 2018; 8: 320-338.
78. Qi J, Sun C, Li D, Zhang H, Yu W, Zebibula A, et al. Aggregation-induced emission luminogen with near-infrared-II excitation and near-infrared-I emission for ultradeep intravital two-photon microscopy. ACS nano. 2018; 12: 7936-7945.
79. Zhu S, Tian R, Antaris AL, Chen X, Dai H. Near-infrared-II molecular dyes for cancer imaging and surgery. Adv Mater. 2019; 31: 1900321.
80. Wu D, Chen L, Lee W, Ko GG, Yin J, Yoon JY. Recent progress in the development of organic dye based near-infrared fluorescence probes for metal ions. Coordin Chem Rev. 2018; 354: 74-97.
81. Xie JY, Li CY, Li YF, Fei J, Xu F, Ou-Yang J, et al. Near-infrared fluorescent probe with high quantum yield and its application in the selective detection of glutathione in living cells and tissues. Anal Chem. 2016; 88: 9746-9752.

82. Guo Z, Park S, Yoon J, Shin I. Recent progress in the development of near-infrared fluorescent probes for bioimaging applications. Chem Soc Rev. 2014; 43: 16-29.
83. Wang K, Du Y, Zhang Z, He KS, Cheng ZQ, Yin L, et al. Fluorescence image-guided tumour surgery. Nat Rev Bioeng. 2023; 1: 161-179.
84. Owens EA, Henary M, El Fakhri G, Choi HS. Tissue-specific near-infrared fluorescence imaging. Acc Chem Res. 2016; 49: 1731-1740.
85. Park JH, Royer JE, Chagarov E, Kaufman-Osborn T, Edmonds M, Kent T, et al. Atomic imaging of the irreversible sensing mechanism of NO2 adsorption on copper phthalocyanine. J Am Chem Soc. 2013; 135: 14600-14609.
86. Zelenka K, Borsig L, Alberto R. Metal complex mediated conjugation of peptides to nucleus targeting acridine orange: a modular concept for dual-modality imaging agents. Bioconjug Chem. 2011; 22: 958-967.
87. Karaman O, Alkan GA, Kizilenis C, Akgul CC, Gunbas G. Xanthene dyes for cancer imaging and treatment: A material odyssey. Coord Chem Rev. 2023; 475: 214841.
88. Khan Z, Sekar N. Far-red to NIR emitting xanthene-based fluorophores. Dyes Pigm. 2023; 208: 110735.
89. Wang GM, Xu WJ, Yang HG, Fu NY. Highly sensitive and selective strategy for imaging Hg2+ using near-infrared squaraine dye in live cells and zebrafish. Dyes Pigm. 2018; 157: 369-376.
90. Xia G, Wang H. Squaraine dyes: The hierarchical synthesis and its application in optical detection. J Photochem Photobiol. 2017; 31: 84-113.
91. He X, Wu X, Wang K, Shi B, Hai L. Methylene blue-encapsulated phosphonate-terminated silica nanoparticles for simultaneous *in vivo* imaging and photodynamic therapy. Biomaterials. 2009; 30: 5601-5609.
92. Qian J, Gong D, Teng Z, Wang J, Cao T, Iqbal K, et al. 2-Vinylfuran substituted BODIPY H2S fluorescent turn on probe based on hydrolysis of furfural and nucleophilic addition of double bond. Sens Actuators B Chem. 2019; 297: 126712.
93. Lu H, Mack J, Yang Y, Shen Z. Structural modification strategies for the rational design of red/NIR region BODIPYs. Chem Soc Rev. 2014; 43: 4778-4823.
94. Li H, Yao Q, Fan J, Du J, Wang J, Peng X. A two-photon NIR-to-NIR fluorescent probe for imaging hydrogen peroxide in living cells. Biosens Bioelectron. 2017; 94: 536-543.
95. Giraldo JP, Landry MP, Kwak SY, Jain RM, Wong MH, Iverson NM, et al. A ratiometric sensor using single chirality near-infrared fluorescent carbon nanotubes: Application to *in vivo* monitoring. Small. 2015; 11: 3973-3984.
96. Wegner K D, Hildebrandt N. Quantum dots: bright and versatile *in vitro* and *in vivo* fluorescence imaging biosensors. Chem Soc Rev. 2015; 44: 4792-4834.
97. Wei Z, Sun L, Liu J, Zhang JZ, Yang H, Yang Y, et al. Cysteine modified rare-earth up-converting nanoparticles for *in vitro* and *in vivo* bioimaging. Biomaterials. 2014; 35: 387-392.
98. Liu Y, Wolstenholme CH, Carter GC, Liu H, Hu H, Grainger LS, et al. Modulation of fluorescent protein chromophores to detect protein aggregation with turn-on fluorescence. J Am Chem Soc. 2018; 140: 7381-7384.
99. Köller A, Grzegorzewski J, Tautenhahn HM, König M. Prediction of survival after partial hepatectomy using a physiologically based pharmacokinetic model of indocyanine green liver function tests. Front Physiol. 2021; 12: 730418.
100. Sakurai N, Ishigaki K, Terai K, Heishima T, Okada K, Yoshida O, et al. Impact of near-infrared fluorescence imaging with indocyanine green on the surgical treatment of pulmonary masses in dogs. Front Vet Sci. 2023; 10: 1018263. .
101. Faruqi R, de la Motte C, Dicorleto PE. Alpha-tocopherol inhibits agonist-induced monocytic cell adhesion to cultured human endothelial cells. J Clin Invest. 1994; 94: 592-600.
102. Nakano H, Oussoultzoglou E, Rosso E, Casnedi S, Chenard-Neu MP, Dufour P, et al. Sinusoidal injury increases morbidity after major hepatectomy in patients with colorectal liver metastases receiving preoperative chemotherapy. Ann Surg. 2008; 247: 118-124.
103. Kim T, Kim BW, Wang HJ, Lee HY, Won JH, Kim J, et al. Quantitative assessment of the portal pressure for the liver surgery using serological tests. Ann Surg. 2016; 264: 330.
104. Landsman ML, Kwant G, Mook GA, Zijlstra WG. Light-absorbing properties, stability, and spectral stabilization of indocyanine green. J Appl Physiol. 1976; 40: 575-583.
105. Desmettre T, Devoisselle JM, Mordon S. Fluorescence properties and metabolic features of indocyanine green (ICG) as related to angiography. Surv Ophthalmol. 2000; 45: 15-27.
106. Ishizawa T, Fukushima N, Shibahara J, Masuda K, Tamura S, Aoki T, et al. Real-time identification of liver cancers by using indocyanine green fluorescent imaging. Cancer. 2009; 115: 2491-2504.
107. Sakoda M, Ueno S, Iino S, Hiwatashi K, Minami K, Kawasaki Y, et al. Anatomical laparoscopic hepatectomy for hepatocellular carcinoma using indocyanine green fluorescence imaging. J Laparoendosc Adv Surg Tech A. 2014; 24: 878-882.
108. Xu C, Cui X, Jia Z, Shen X, Che J. A meta-analysis of short-term and long-term effects of indocyanine green fluorescence imaging in hepatectomy for liver cancer. Photodiagnosis Photodyn Ther. 2023; 42: 103497.
109. Zhu G, Qiu X, Zeng L, Zou Z, Yang L, Nie S, et al. Application of indocyanine green-mediated fluorescence molecular imaging technology in liver tumors resection: a systematic review and meta-analysis. Front Oncol. 2023; 13: 1167536.
110. Wang J, Xu Y, Zhang Y, Tian H. Safety and effectiveness of fluorescence laparoscopy in precise hepatectomy: A meta-analysis. Photodiagnosis Photodyn Ther. 2023; 42: 103599.
111. Wakabayashi T, Cacciaguerra AB, Abe Y, Bona ED, Nicolini D, Mocchegiani F, et al. Indocyanine green fluorescence navigation in liver surgery. Ann Surg Oncol. 2022; 275: 1025-1034.
112. van Oosterom MN, van Leeuwen SI, Mazzone E, Dell'Oglio P, Buckle T, van Beurden F, et al. Click-on fluorescence detectors: using robotic surgical instruments to characterize molecular tissue aspects. J Robot Surg. 2023; 17: 131-140.
113. Azargoshasb S, Boekestijn I, Roestenberg M, KleinJan GH, van der Hage JA, van der Poel HG, et al. Quantifying the impact of signal-to-background ratios on surgical discrimination of fluorescent lesions. Mol Imaging Biol. 2023; 25: 180-189.
114. Smith AM, Mancini MC, Nie S. Second window for *in vivo* imaging. Nat Nanotechnol. 2009; 4: 710-711.
115. Hu Z, Fang C, Li B, Zhang Z, Cao C, Cai M, et al. First-in-human liver-tumour surgery guided by multispectral fluorescence imaging in the visible and near-infrared-I/II windows. Nat Biomed Eng. 2019; 4: 259-271.
116. Li C, Wang Q. Challenges and opportunities for intravital near-infrared fluorescence imaging technology in the second transparency window. ACS nano. 2018; 12: 9654-9659.
117. Antaris AL, Chen H, Cheng K, Sun Y, Hong G, Qu C, et al. A small-molecule dye for NIR-II imaging. Nat Mater. 2015; 15: 235-242.
118. Zhang P, Wu Q, Yang J, Hou M, Zheng B, Xu J, et al. Tumor microenvironment-responsive nanohybrid for hypoxia amelioration with photodynamic and near-infrared II photothermal combination therapy. Acta Biomater. 2022; 146: 450-464.
119. Zhu S, Hu Z, Tian R, Yung BC, Yang Q, Zhao S, et al. Repurposing cyanine NIR-I dyes accelerates clinical translation of near-infrared-II (NIR-II) bioimaging. Adv Mater. 2018; 30: 1802546.
120. Carr JA, Franke D, Caram JR, Perkinson CF, Saif M, Askoxylakis V, et al. Shortwave infrared fluorescence imaging with the clinically approved near-infrared dye indocyanine green. Proc Natl Acad Sci U S A. 2018; 115: 4465-4470.
121. Zhang YQ, Liu WL, Luo XJ, Shi JP, Zeng YZ, Chen WL, et al. Novel self-assembled multifunctional nanoprobes for second-near-infrared-fluorescence-image-guided breast cancer surgery and enhanced radiotherapy efficacy. Adv Sci. 2023; 10: e2205294.
122. Starosolski Z, Bhavane R, Ghaghada KB, Vasudevan SA, Kaay A, Annapragada A. Indocyanine green fluorescence in second near-infrared (NIR-II) window. PLoS One. 2017; 12: e187563.
123. Zhu B, Sevick-Muraca EM. A review of performance of near-infrared fluorescence imaging devices used in clinical studies. Br J Radiol. 2015; 88: 20140547.
124. Wu Y, Suo Y, Wang Z, Yu Y, Duan S, Liu H, et al. First clinical applications for the NIR-II imaging with ICG in microsurgery. Front Bioeng Biotechnol. 2022; 10: 1042546.
125. Li Z, Li Z, Ramos A, Boudreaux JP, Thiagarajan R, Mattison YB, et al. Detection of pancreatic cancer by indocyanine green-assisted fluorescence imaging in the first and second near-infrared windows. Cancer Commun. 2021; 41: 1431-1434.
126. Cao C, Deng S, Wang B, Shi X, Ge L, Qiu M, et al. Intraoperative near-infrared II window fluorescence imaging-assisted nephron-sparing surgery for complete resection of cystic renal masses. Clin Transl Med. 2021; 11: e604.
127. Shi X, Zhang Z, Zhang Z, Cao C, Cheng Z, Hu Z, et al. Near-infrared window II fluorescence image-guided surgery of high-grade gliomas prolongs the progression-free survival of patients. IEEE Trans Biomed Eng. 2022; 69: 1889-1900.
128. Shen B, Zhang Z, Shi X, Cao C, Zhang Z, Hu Z, et al. Real-time intraoperative glioma diagnosis using fluorescence imaging and deep convolutional neural networks. Eur J Nucl Med Mol Imaging. 2021; 48: 3482-3492.
129. Wu H, Wang MD, Zhu JQ, Li ZL, Wang WY, Gu LH, et al. Mesoporous nanoparticles for diagnosis and treatment of liver cancer in the era of precise medicine. Pharmaceutics. 2022; 14: 1760.
130. Zhao XH, Li HL, Guo CY, Yao QJ, Xia WL, Hu HT. Downstaging and conversation strategy for advanced hepatocellular carcinoma with portal vein branch tumor thrombus: TACE, 125I seed implantation, and RFA for hepatocellular carcinoma with portal vein branch tumor thrombus. J Hepatocell Carcinoma. 2023; 10: 231-240.
131. He P, Zhong F, Luo B, Luo G, Wang X, Xia X, et al. Super-stable homogeneous iodinated formulation technology for improving the therapeutic effect of patients with advanced hepatocellular carcinoma. Quant Imaging Med Surg. 2020; 10: 2223-2226.
132. Xu Y, Chen M, Meng X, Lu P, Wang X, Zhang W, et al. Laparoscopic anatomical liver resection guided by real-time indocyanine green fluorescence imaging: experience and lessons learned from the initial series in a single center. Surg Endosc. 2020; 34: 4683-4691.
133. Li WF, Al-Taher M, Yu CY, Liu YW, Liu YY, Marescaux J, et al. Super-selective intra-arterial indocyanine green administration for near-infrared fluorescence-based positive staining of hepatic segmentation: A feasibility study. Surg Innov. 2021; 28: 669-678.
134. Zhang Y, Cheng H, Chen H, Xu P, Ren E, Jiang Y, et al. A pure nanoICG-based homogeneous lipiodol formulation: toward precise surgical navigation of

primary liver cancer after long-term transcatheter arterial embolization. Eur J Nucl Med Mol Imaging. 2022; 49: 2605-2617.
135. He P, Xiong Y, Ye J, Chen B, Cheng H, Liu H, et al. A clinical trial of super-stable homogeneous lipiodol-nanoICG formulation-guided precise fluorescent laparoscopic hepatocellular carcinoma resection. J Nanobiotechnology. 2022; 20: 250.
136. Wang Z, Yang F, Zhao X, Mi J, Sun L, Kang N, et al. Outcome of near-infrared fluorescence-navigated pulmonary metastasectomy for hepatocellular carcinoma. Eur J Cardiothorac Surg. 2022; 62: ezac270.
137. Xia Y, Xu C, Zhang X, Ning P, Wang Z, Tian J, et al. Liposome-based probes for molecular imaging: from basic research to the bedside. Nanoscale. 2019; 11: 5822-5838.